In$_{1-x}$Ga$_x$As Double Metal Gate-Stacking Cylindrical Nanowire MOSFET for highly sensitive Photo detector

Sanjeev Kumar Sharma[a], Parveen Kumar[b], Balwant Raj[c] and Balwinder Raj[d]

[a,b] Department of Electronic and Communication Engineering,
Dr. B. R. Ambedkar National Institute of Technology, Jalandhar-144011, India
[c]Department of Electronic and communication Engineering, PUSSGRC, Hoshiarpur, Punjab
[d]Department of Electronic and Communication Engineering,
National Institute of Technical Teachers Training and Research, Chandigarh-160019, India
[*]**Correspondance to** sanjeev.nitj14@gmail.com

Abstract:

This paper proposed a highly sensitive Double Metal Gate-stacking Cylindrical Nanowire-MOSFET (DMG CL-NWMOSFET) photosensor by using In$_{1-x}$Ga$_x$As. For the best control of short channel effects (SCEs), a double metal gate has been utilized and for efficient photonic absorption, III-V compound has been utilized as channel material. The currently available Conventional Filed-Effect-Transistors (CFET) based photosensor have been used threshold voltage as parameter for the calculation of sensitivity, but in the proposed photosensor, change in subthreshold current has been used as the detecting parameters for sensitivity ($I_{illumination}/I_{dark}$). The scientifically electrons study and the photo-conductive characteristics of In$_{1-x}$Ga$_x$As CL-NWMOSFET are taken through Silvaco Atlas Tools. After the analysis of In$_{1-x}$Ga$_x$As dual Metal Gate Stacking Cylindrical NWMOSFET responds to detectable spectrum (~ 450 nm), incidents light with constant, reversible and fast response by responsivity (4.3 mAW^{-1}), high $I_{illumination}/I_{dark}$ (1.36 * 10^9) and quantum-efficiency (1.12 %). The obtained results of In$_{1-x}$Ga$_x$As DMG CL-NWMOSFET based photodetectors have the potential in optoelectronics applications.

Keywords: NWMOSFET, Dark current, Quantum efficiency (Q_e), Responsivity, Photo-sensor.

1. Introduction

Nanowires (NW) comprises of Indium gallium arsenide (InGaAs) is favorable semiconductor material due to its excellent properties such as emission wavelength over large spectral ranges, tunable band gap, variable Schottky barrier heights, high saturation velocities, one dimensional conduction, with high absorption coefficients [1–3] and it additionally gives epitaxial combination on silicon substrate [4–7]. In current Nanoscale industry, huge number of electronic and photonic devices is designing based on devices such as photonic crystal laser [8], nanolasers [9], light-emitting diodes (LED) [10], and solar cells [11], as well as tunnel diodes [12] and short channel three dimensional (3D) transistors [13]. The photosensor based on Metal Oxide Semiconductor Field Effect Transistor (MOSFET) [14]and Metal Semiconductor Field Effect Transistor (MESFET) have variety of merits such as high input impedance, low power dissipation and low noise as well as its high stability towards temperature as compared to the conventional photodetectors such as pn junction photodiode, avalanche photodiode and pin photodiode. The main drawback of pn junction based photodiode is having low-quantum efficiency, but pin photodiode is faster than pn photodiode with high sensitivity [15], but its speed of operation is limited by transit time (T_t) of photogenerated carriers. Similarly, high sensitivity can be also achieved using Avalanche photodiode, but it faces the problem of higher noise [16]. Nowadays, CMOS based image sensors is mostly used due to various merits such as

random sensor, low power-consumption, and design flexibility [17–19]. MOSFET is better as compared to MESFET due to its integration methodology and promising device due low power consumption and low Dark Current (I_{dark}). Further, dark current can also reduces using non planar devices like Cylindrical (CL) gate MOSFET, because of better gate control as compared to single gate (SG) bulk MOS transistors.

This paper presents a highly sensitive Double Metal Gate Stacking Cylindrical Nanowire (NW) MOSFET photosensor by using $In_{1-x}Ga_xAs$ including the Double Metal Gate and III-V compound has been utilized as channel material. The different metal work function has been used for better carrier transport proficiency and designing of CL-NWMOSFET. The higher work-function has been utilized to accelerate the charge carrier in the channel [20–22] and lower work-function at drain side for the reduction of peak electric field , which also results in reduced Hot -Carrier-Effect [23]. To fulfill the requirement of effective absorption of light in the desired spectrum, III-V compound material has been used as the channel material such as InGaAs. InGaAs has absorbed light more efficiently, due to director bandgap material as compared to indirect bandgap materials. In this present work, photosensor has been biased in subthreshold area as reported in [24] , which results in realizing highly sensitive photodetector based on low power.

2. Device Structure

The designed 3D view of DMG CL-NWMOSFET structure under incident radiation is shows in Figure 1 (a) and cross-sectional view in Figure 1 (b). The dimensional parameters such as channel/gate length (L), source/drain length are taken as 20 nm and diameter (D) taken as 5nm. The maintained the Equivalent Oxide Thickness (EOT) in the DMG CL-NWMOSFET designing, high-k and low-k materials such as HfO_2 and SiO_2 respectively are used for gate stacking [25] as well as the value of EOT is taken as 0.8 nm. The film of III-V material such as $In_{.53}Ga_{.47}$ is kept lightly doped/undoped for the reduction of mobility degradation. The gate work-function of metal 1 (Φ_{M1}), near source at L1 is higher than the gate work function of metal 2 (Φ_{M2}), near drain at L2 ($\Phi_{M1} > \Phi_{M2}$). The total channel/gate length is equal to summation of L1 and L2.

(a)
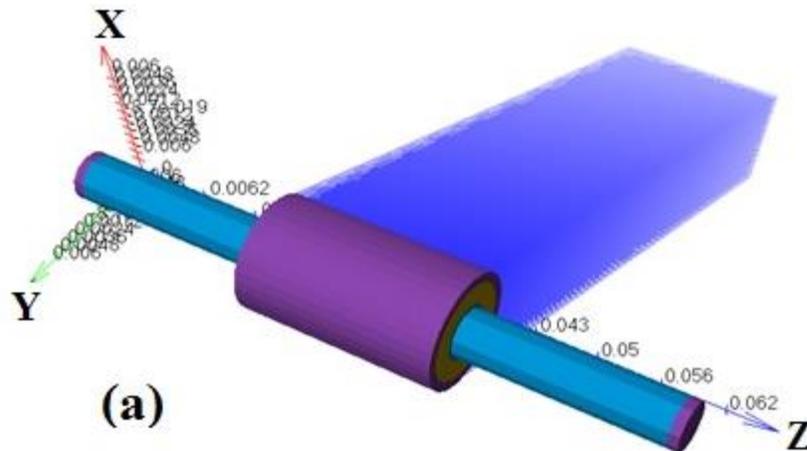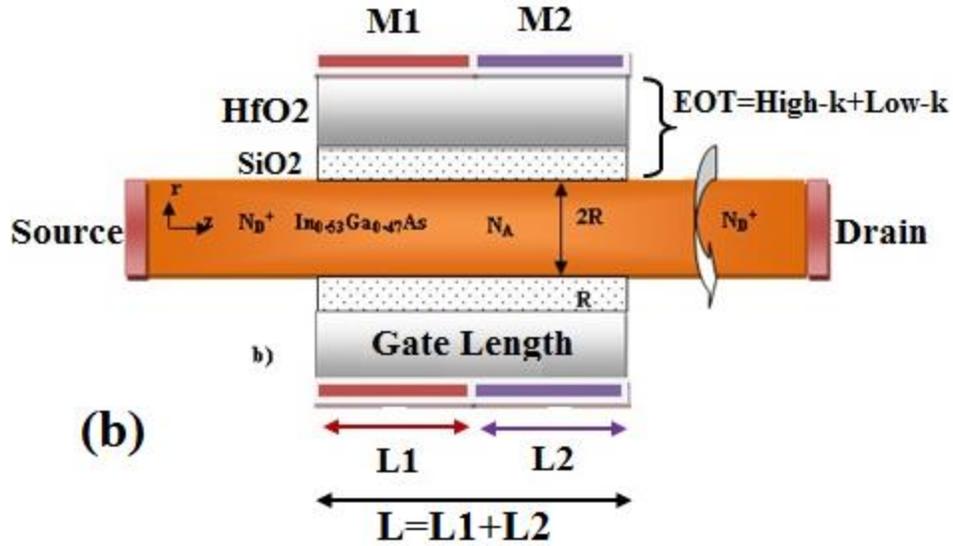
Figure. 1 (a) Three dimensional view of DMG CL-NWMOSFET (b) Cross-section view of DMG CL-NWMOSFET

3. Simulation methodology

Model used:

The various models are used for simulation of DMG CL-NWMOSFET, such as Shockey Read Hall (SRH) [26] for generation and recombination of carrier, Bohm Quantum Model (BQP) for quantum mechanical effect, which cannot be ignored in Nanoscale [27]. In BQP model the values of alpha and gamma are taken as 0.5 and 1.2 respectively [28]. The physical parameters of DMG CL-NWMOSFET are illustrates in Table 1.

**Table 1 Parameters of DMG CL-NWMOSFET**

Parameters	Value
Nanowire Diameter (D)	05 nm
Channel/Gate length (L)	20 nm
EOT	0.8 nm
Thickness of Low-k material (SiO_2)	0.4 nm
Thickness of Hihg-k material (HfO_2)	2.1 nm
$In_{1-x} Ga_x As$	x=0.47
Source/drain length	20 nm
Drain-Source Voltage (V_{ds})	0.1 V
Permittivity of Low-k material	3.9
Permittivity of High-k material	21
Work-function of metal 1 (Φ_{M1})	4.83 eV
Work-function of metal 2 (Φ_{M2})	4.41 eV

Method used:

The block method has been used for numerical solution during to simulation process of In$_{1-x}$Ga$_x$As Double Metal Gate Stacking Cylindrical Nanowire-MOSFET.

Calibration with reported paper:

The simulation results of the In$_{0.53}$Ga$_{0.47}$As DMG CL-NWMOSFET are validated using Silvaco TCAD simulator with the reported research paper [29] for different parameters such as channel/gate length (L), oxide thickness (t$_{ox}$), gate work function (Φ), radius of Nanowire (R), channel doping (N$_A$) and source/drain doping (N$_D^+$) are taken as 1 μm, 1.5 nm, 5.05 eV, 7.5 nm, $1e^{14}$ cm^{-3} and $5e^{17}$ cm^{-3} respectively at V$_{gs}$-V$_t$=0.5, where as V$_{gs}$ respresents the gate-source voltage and V$_t$ represents the threshold voltage. The extraction of data has been performed by graph digitizer and plotted with simulated results. The result shows that the better agreement with reference [29]. The calibration curve of DMG CL-NWMOSFET with reported data are shown in Figure 2.
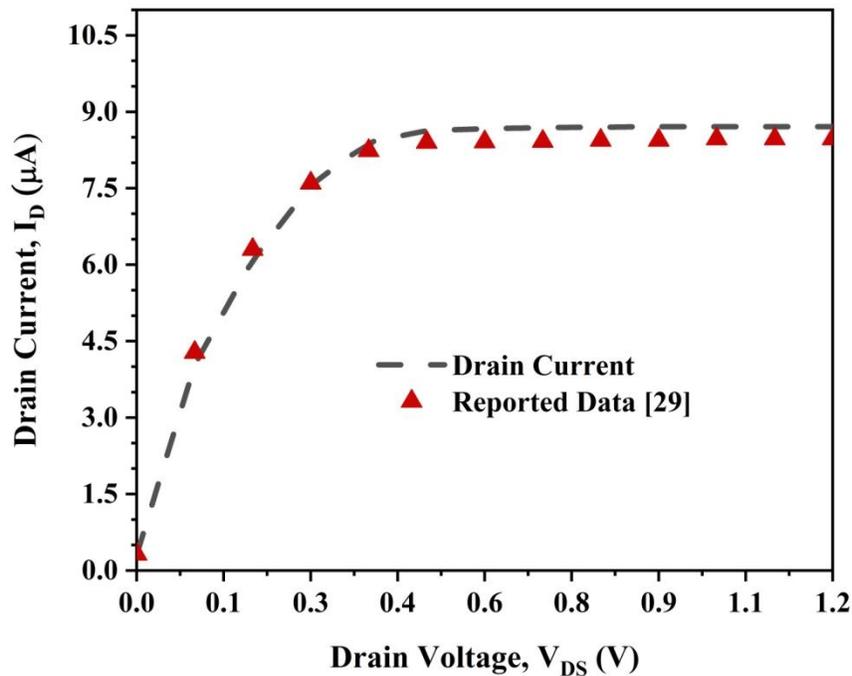
Figure 2. Calibration Curve of DMG CL-NWMOSFET with Reported data [29].

The structure of DMG CL-NWMOSFET has been designed by using Silvaco Atlas 3D simulator. The metal work-function of source side (Φ_{M1}) and drain side (Φ_{M2}) are taken as 4.83 eV and 4.41 eV respectively. The work-function has been tuned to get required threshold voltage (V$_t$). The Gate Drive Voltage (Vgt) is the important factor for defining the region of operation, which is equal to Vgt = V$_{gs}$-V$_t$.

Optical Beam

In order to archive the accurate characteristics of device under dark/ incident radiations are obtained through SILVACO tools (3D). To calculate the photo generation rate at defined meshing points, advance optical device simulator (LUMINOUS-3D) incorporates under the incident radiation with the help of Ray Trace method. The parameters of DMG CL-

NWMOSFET which is utilized for simulation work are given in Table 1. The various optical parameters such as wavelength, location and radiation intensity for incident radiation are located by using BEAM keyword, which is incorporated in optical simulator module that is LUMINOUS-3D.

4. Result and Discussion

To study the performance of $In_{0.53}Ga_{0.47}As$ DMG CL-NWMOSFET as a photosensor application, the device has been presented with monochromatic beam of light in vertical nature and corresponding results are recorded. Figure 3 represents the drain current (I_d) variation with respect to gate-source voltage (V_{gs}) of $In_{0.53}Ga_{0.47}As$ DMG CL-NWMOSFET under dark and illuminated conditions with different light intensity and incident power (P_i) respectively, by taking wavelength (λ) is equal to 0.450 µm, EOT = 1.2 nm and $N_A= 1\times10^{16}$ cm^{-}3 at drain-source voltage (V_{ds}) is equal to 0.1 V. If the value of incident power is increases, then the generation of electron-hole pair increases which also increases the conductivity of the channel ($In_{0.53}Ga_{0.47}As$) under incident power (P_i).Due to effect of photo-gating and photo-dopping [30] higher current are obtained under incident radiations. This change in illumination current ($I_{illumination}$) with respect to power changes is more suitable in subthreshold area as compared to other regions such as linear and saturation. hence proposed $In_{0.53}Ga_{0.47}As$ DMG CL-NWMOSFET works good agreement as a ultraviolet visible photosensor in this area like subthrehold area/region. According to Figure 3, it is clear that if the power increases from picowatts (pW) towards microwatts (µW), the photocurrent increases and maximum saturation are obtained at P_i=16.5 µW. The further increase in power after this value, the performance of the proposed device has been degraded and also consumes more power during their operation.
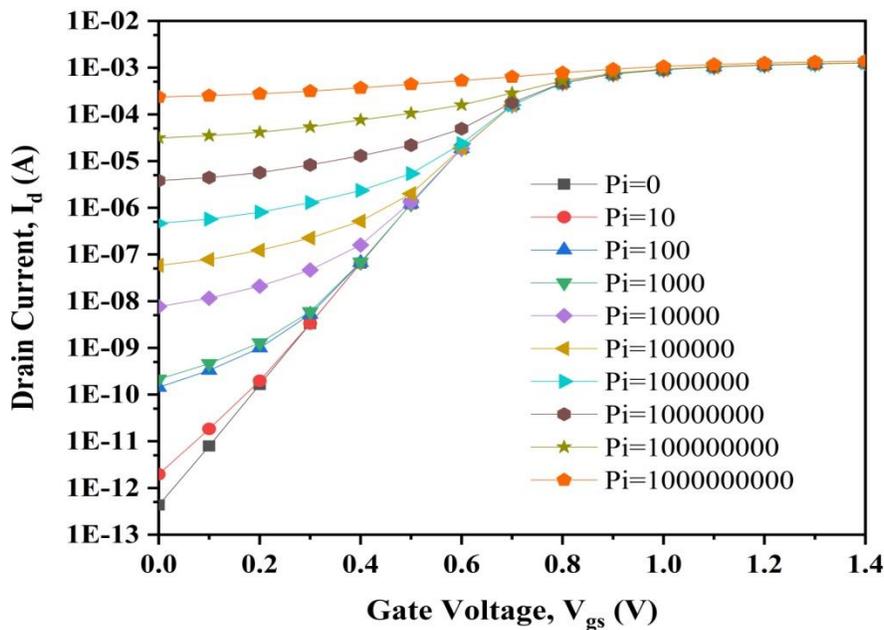
Figure. 3 Characteristics (VI) curve of $In_{0.53}Ga_{0.47}As$ DMG CL-NWMOSFET under illumination-condition for

various values of incident power (P_i)
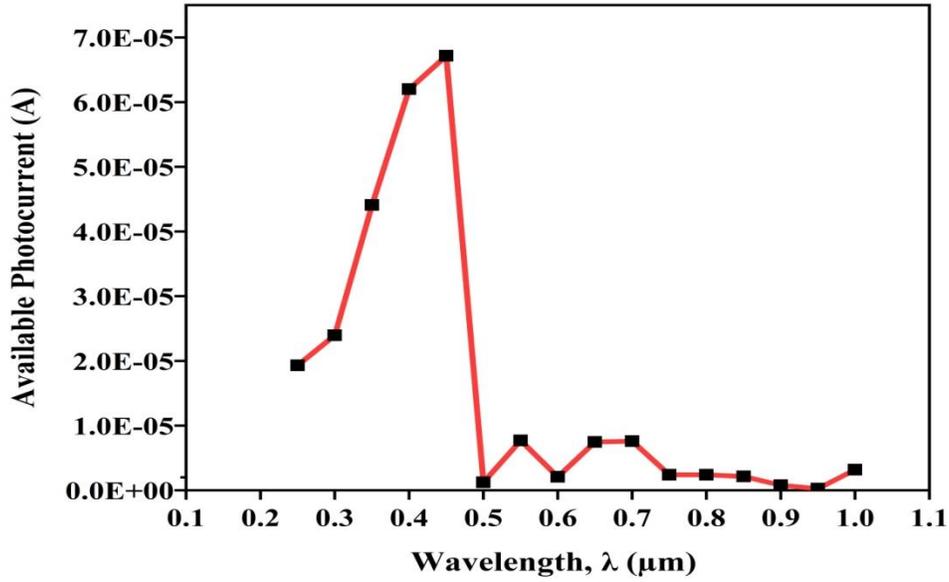
Figure. 4 Curve between Available Photocurrent (I_{ap}) and Wavelength (λ) of $In_{0.53}Ga_{0.47}As$ DMG CL-NWMOSFET under illumination with P_i= 16.5 µW at V_{ds}=0.1 V

Figure 4 shows the curve between available photocurrent (I_{ap}) and wavelength (λ) under illumination by taking L=20 nm, radius of Nanowire (R) = 2.5 nm, $N_A = 1 \times 10^{16}$ cm^{-3} and fixed incident power (P_i) = 16.5 µW. The data extraction has been performed at V_{gs} = 0.0 V, V_{ds}=0.1 V, EOT= 1.2 nm, and obtained maximum available photocurrent (I_{ap}). According to Figure 4, the peak value of I_{ap} has observed around λ= 0.450 µm, because of at this λ value maximum light is absorbed from source to channel that is $In_{0.53}Ga_{0.47}As$. Another two important parameters such as Responsivity (Re) and Quantum Efficiency (Qe) can be evaluated by using following formula as shown in equation (1) and (2) respectively for photosensor application.

$$\text{Responsivity } (R_e) = \frac{\text{Available Photocurrent,} I_{ap} \text{ (Ampere)}}{\text{Incident Optical Power,} P_i \text{ (Watt)}} \tag{1}$$
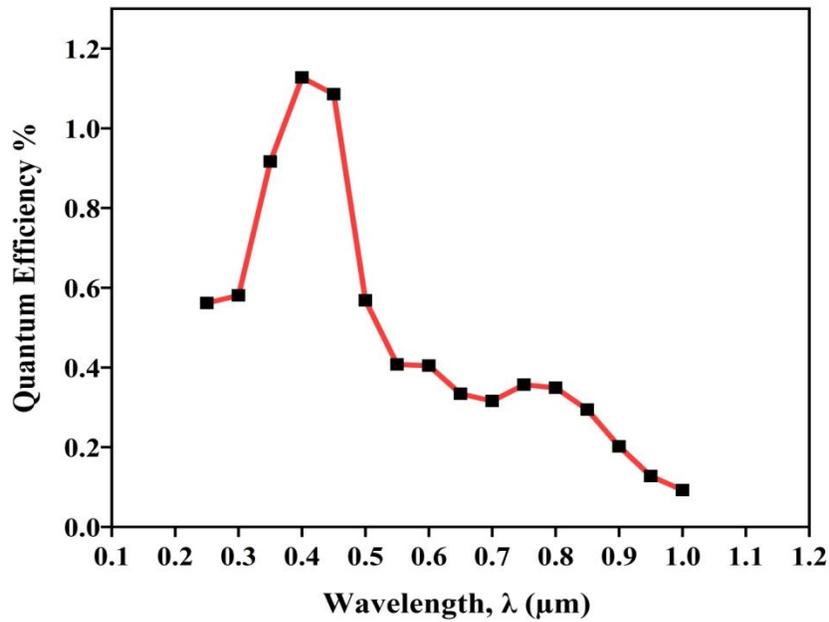
$$\text{Quantum Efficiency } (Q_e) = R_e \times \frac{hc}{q\lambda} \tag{2}$$

Figure. 5 shows the responsivity (R_e) of the of proposed device with wavelength ranging from 0.0 µm to 1.2 µm by taking same parametric values which are used to calculate the $I_{ap;}$ with different values of work-function for metal 1(Φ_{M1}) and metal 2 (Φ_{M2}) such as 4.83 eV and 4.41 eV respectively. The peak value of R_e has been observed at wavelength (λ) = 0.450 µm and it lies in the visible region of spectrum as shown in Figure 5. Hence, proposed DMG CL-NWMOSFET works powerfully as a visible photodetector, which is highly recommended for various biological and sensing applications [31, 32].
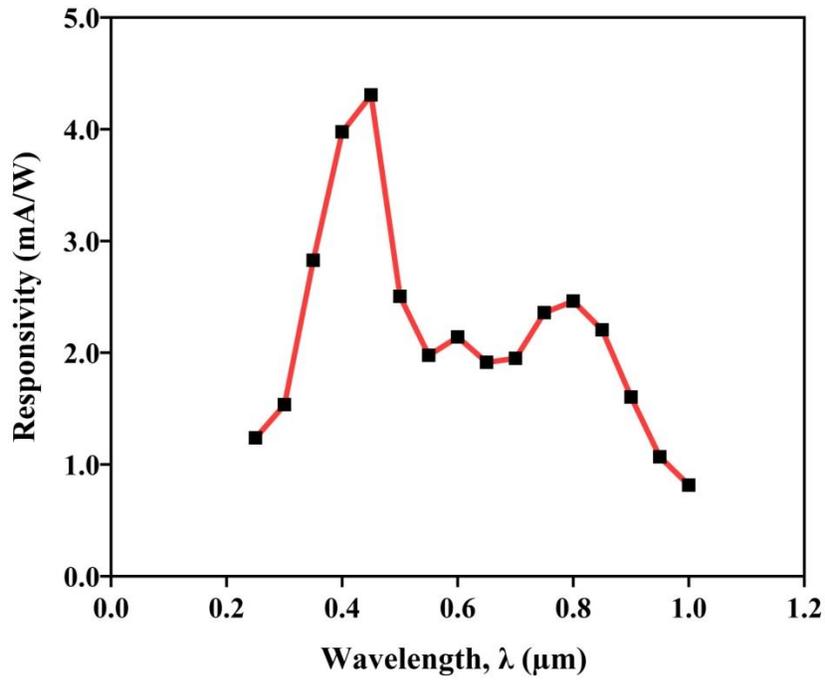
Figure. 5 Responsivity (Re) vs Wavelength (λ) curve of DMG CL-NWMOSFET

Figure. 6 show the curve between percentage Quantum Efficiency (Q_e) and different wavelength (λ) of the channel. It is observed that the value of Q_e increases with the increase in λ from 0.2 μm to 0.45 μm. If the value of λ increases from 0.45 μm, then percentage Q_e decreases with the increase in λ for R= 2.5 nm at V_{gs} = 0.0 V, V_{ds}=0.1 V. Hence the carefully Quantum Efficiency first increases with increase in wavelengths and then decreases after attaining a maximum value at λ=0.450 μm for R=2.5 nm. Hence DMG CL-NWMOSFET can be utilized as a vastly efficient photosensor in visible range of spectrum.


Figure. 6 Curve between percentage Quantum Efficiency (Q_e) and Wavelength (λ) of DMG CL-NWMOSFET

The sensitivity (S) is the important parameter of photodetector and it is defined as the ratio of obtained current under illumination ($I_{illumination}$) to dark condition (I_{dark}) as shown in equation (3).

$$\text{Sensitivity (S)} = \frac{\text{Current under Illumination } (I_{illumination})}{\text{Current under dark } (I_{dark})} \tag{3}$$

The sensitivity (S) versus incident Wavelength (λ) curve of proposed device under illumination is shown in Figure. 7. The data extraction has been performed at $V_{gs} = 0.0$ V, $V_{ds}=0.1$ V, EOT= 1.2 nm with physical parameters of proposed device such as L=20 nm, radius of Nanowire (R) = 2.5 nm, $N_A = 1\times10^{16}$ cm^{-3}, $\Phi_{M1} = 4.83$ eV, $\Phi_{M2} = 4.41$ eV and fixed incident power (P_i) = 16.5 µW. It is observed that the value of S is small at lower spectrum and maximum at near about 0.45value of λ. After crossing the λ=0.45, the sensitivity further decreases at higher spectrum. Hence the proposed DMG CL-NWMOSFET can be effectively utilized as a highly sensitive low power photosensor in visible region of spectrum.
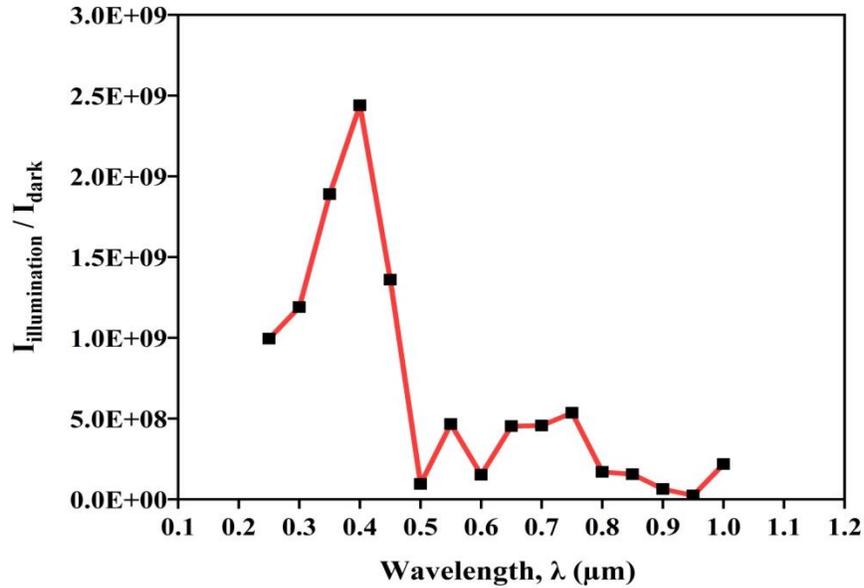
Figur. 7 Sensitivity (S) versus Wavelength (λ) curve for DMG CL-NWMOSFET

5. Conclusion

The device DMG CL-NWMOSFET has been successfully demonstrated with single In$_{0.53}$Ga$_{0.47}$As Nanowire (NW) and analyses photoelectric performances of the device. The proposed In$_{1-x}$Ga$_x$As Double Metal Gate-stacking Cylindrical Nanowire-MOSFET has efficiently responds to near about 0.45 µm in terms of visible spectrum incident light with stable and fast response. After the variation of different parameters with respect to wavelength, the best optimum value for responsivity (R_e), Quantum efficiency (Q_e) and high photo Sensitivity (S) are observed such as 4.3 mAW^{-1}, 1.12% and 1.36x10^9 respectively. The performance and characteristics of DMG CL-NWMOSFET has been better than conventional detectors based on telluride, selenide and sulfide. Although, In$_{0.53}$Ga$_{0.47}$As NW structure based on one-dimensional

(1D) have been improved significantly, but many challenges have reside. Exact control of NW width, including imperfections, traps and surface states for basically building up reliable devices.

Funding statement:

Conflict of Interest:

Authors declare that there is no conflict of Interest.

Author contributions:

- Highly sensitive Double Metal Gate-stacking Cylindrical Nanowire-MOSFET (DMG CL-NWMOSFET) photosensor by using $In_{1-x}Ga_xAs$.
- A double metal gate has been utilized and for efficient photonic absorption, III-V compound has been utilized as channel material.
- Proposed photosensor, change in subthreshold current has been used as the detecting parameters for sensitivity ($I_{illumination}/I_{dark}$).
- The scientifically electrons study and the photo-conductive characteristics of $In_{1-x}Ga_xAs$ CL-NWMOSFET are taken through Silvaco Atlas Tools.
- The analysis of $In_{1-x}Ga_xAs$ dual Metal Gate Stacking Cylindrical NWMOSFET responds to detectable spectrum (~ 450 nm), incidents light with constant, reversible and fast response by responsively (4.3 mAW^{-1}), high $I_{illumination}/I_{dark}$ (1.36 * 10^9) and quantum-efficiency (1.12 %).
- The results of $In_{1-x}Ga_xAs$ DMG CL-NWMOSFET based photodetectors have the potential in optoelectronics applications.

Availability of data and material:

Data used for the results are available in the manuscript

Compliance with ethical standards:

Not applicable

Consent to participate:

We here give our consent to participate and communicate paper in this journal.

Consent for Publication:

We here give our consent to publish paper in this journal.

Acknowledgment

References

1. Koblmüller G, Abstreiter G (2014) Growth and properties of InGaAs nanowires on silicon. Phys status solidi (RRL)–Rapid Res Lett 8:11–30

2. Kumar P, Sharma SK (2020) Comparative Analysis of Nanowire Tunnel Field Effect Transistor for Biosensor Applications. Silicon 1–8

3. Sharma SK, Singh J, Raj B, Khosla M (2018) Analysis of Barrier Layer Thickness on Performance of In1–x Ga x As Based Gate Stack Cylindrical Gate Nanowire MOSFET. J Nanoelectron Optoelectron 13:1473–1477

4. Tomioka K, Tanaka T, Hara S, et al (2010) III–V nanowires on Si substrate: selective-area growth and device applications. IEEE J Sel Top Quantum Electron 17:1112–1129

5. Shin JC, Kim KH, Yu KJ, et al (2011) In x Ga1-x As nanowires on silicon: One-dimensional heterogeneous epitaxy, bandgap engineering, and photovoltaics. Nano Lett 11:4831–4838

6. Hertenberger S, Funk S, Vizbaras K, et al (2012) High compositional homogeneity in In-rich InGaAs nanowire arrays on nanoimprinted SiO2/Si (111). Appl Phys Lett 101:43116

7. Hou JJ, Han N, Wang F, et al (2012) Synthesis and characterizations of ternary InGaAs nanowires by a two-step growth method for high-performance electronic devices. ACS Nano 6:3624–3630

8. Singh A, Khosla M, Raj B (2017) Analysis of electrostatic doped Schottky barrier carbon nanotube FET for low power applications. J Mater Sci Mater Electron 28:1762–1768

9. Chen R, Tran T-TD, Ng KW, et al (2011) Nanolasers grown on silicon. Nat Photonics 5:170–175

10. Dimakis E, Jahn U, Ramsteiner M, et al (2014) Coaxial multishell (In, Ga) As/GaAs nanowires for near-infrared emission on Si substrates. Nano Lett 14:2604–2609

11. Shin JC, Mohseni PK, Yu KJ, et al (2012) Heterogeneous integration of InGaAs nanowires on the rear surface of Si solar cells for efficiency enhancement. ACS Nano 6:11074–11079

12. Yang T, Hertenberger S, Morkötter S, et al (2012) Size, composition, and doping effects on In (Ga) As nanowire/Si tunnel diodes probed by conductive atomic force microscopy. Appl Phys Lett 101:233102

13.   Tomioka K, Yoshimura M, Fukui T (2012) A III–V nanowire channel on silicon for high-performance vertical transistors. Nature 488:189–192

14.   Sharma SK, Raj B, Khosla M (2019) Enhanced photosensitivity of highly spectrum selective cylindrical gate I n 1− x G ax A s nanowire MOSFET photodetector. Mod Phys Lett B 33:1950144

15.   Jain N, Raj B (2016) An analog and digital design perspective comprehensive approach on Fin-FET (fin-field effect transistor) technology—A review. Rev Adv Sci Eng 5:123–137

16.   Stoykov A, Scheuermann R (2004) Silicon avalanche photodiodes. Lab Muon Spin Spectrosc Paul Scherrer Inst

17.   Fossum ER (1993) Active pixel sensors: Are CCDs dinosaurs? In: Charge-Coupled Devices and Solid State Optical Sensors III. International Society for Optics and Photonics, pp 2–14

18.   Schanz M, Brockherde W, Hauschild R, et al (1997) Smart CMOS image sensor arrays. IEEE Trans Electron Devices 44:1699–1705

19.   Cheng H-Y, King Y-C (2003) A CMOS image sensor with dark-current cancellation and dynamic sensitivity operations. IEEE Trans Electron Devices 50:91–95

20.   Gallo EM, Chen G, Currie M, et al (2011) Picosecond response times in GaAs/AlGaAs core/shell nanowire-based photodetectors. Appl Phys Lett 98:241113

21.   Sharma S, Raj B, Khosla M (2016) Comparative Analysis of MOSFET CNTFET and NWFET for High Performance VLSI Circuit Design. A Rev J VLSI Des Tools Technol 6:19–32

22.   Ashima DV, Raj B Performance Analysis of Channel and Inner Gate Engineered GAA Nanowire FET

23.   Jain A, Sharma SK, Raj B (2016) Design and analysis of high sensitivity photosensor using Cylindrical Surrounding Gate MOSFET for low power applications. Eng Sci Technol an Int J 19:1864–1870

24.   Sharma SK, Raj B, Khosla M (2017) Subthreshold Performance of In 1–x Ga x As Based Dual Metal with Gate Stack Cylindrical/Surrounding Gate Nanowire MOSFET for Low Power Analog Applications. J Nanoelectron Optoelectron 12:171–176

25.   Chaturvedi P, Kumar MJ (2014) Impact of gate leakage considerations in tunnel field effect transistor design. Jpn J Appl Phys 53:74201

26.   Shockley W, Read Jr WT (1952) Statistics of the recombinations of holes and electrons. Phys Rev 87:835

27.   Chaudhry A, Roy JN (2010) MOSFET models, quantum mechanical effects and modeling approaches: a review. JSTS J Semicond Technol Sci 10:20–27

28.   Jena B, Ramkrishna BS, Dash S, Mishra GP (2016) Conical surrounding gate MOSFET: a possibility in gate-all-around family. Adv Nat Sci Nanosci Nanotechnol 7:15009

29.   Marin EG, Ruiz FG, Schmidt V, et al (2015) Analytic drain current model for III–V

cylindrical nanowire transistors. J Appl Phys 118:44502

30. Dai X, Zhang S, Wang Z, et al (2014) GaAs/AlGaAs nanowire photodetector. Nano Lett 14:2688–2693

31. Omnès F, Monroy E, Muñoz E, Reverchon J-L (2007) Wide bandgap UV photodetectors: A short review of devices and applications. In: Gallium Nitride Materials and Devices II. International Society for Optics and Photonics, p 64730E

32. Liu K, Sakurai M, Aono M (2010) ZnO-based ultraviolet photodetectors. Sensors 10:8604–8634